Path Integral Treatment of Proton Transport Processes in $BaZrO_3$

Qianfan Zhang,[1] Göran Wahnström,[2,*] Mårten E. Björketun,[2,3] Shiwu Gao,[1,4] and Enge Wang[1]

[1]*State Key Laboratory for Surface Physics, Institute of Physics, Chinese Academy of Sciences, Beijing 100190, China*
[2]*Department of Applied Physics, Chalmers University of Technology, SE-412 96 Göteborg, Sweden*
[3]*Department of Physics, Technical University of Denmark, DK-2800 Lyngby, Denmark*
[4]*Department of Physics, Göteborg University, SE-405 30 Göteborg, Sweden*

(Received 18 June 2008; revised manuscript received 19 September 2008; published 20 November 2008)

Nuclear quantum effects on proton transfer and reorientation in $BaZrO_3$ is investigated theoretically using the *ab initio* path-integral molecular-dynamics simulation technique. The result demonstrates that adding quantum fluctuations has a large effect on, in particular, the transfer barrier. The corresponding rates and diffusion coefficient are evaluated using the path-centroid transition state theory. In contrast with what is found assuming classical mechanics for the nuclear motion, the reorientation step becomes rate limiting below 600 K.

DOI: 10.1103/PhysRevLett.101.215902 PACS numbers: 66.30.jp, 63.20.dk, 66.35.+a

Proton conduction is a ubiquitous phenomenon, influencing dynamical behavior in a wide variety of systems ranging from materials science to biochemistry. Several perovskite-type oxides with the general formula ABO_3 exhibit significant proton conductivity at elevated temperatures and are potential candidates as electrolyte materials in various electrochemical applications [1]. Apart from being of technological importance, they also serve as model systems for fast proton transport in solids [2]. Basically, the long-range proton migration in these oxides occurs as a sequence of hydrogen-bond mediated proton transfers (T) between neighboring lattice oxygens and reorientations (R) around the same oxygen site [3]. A system particularly well suited for studying the elementary diffusional steps is $BaZrO_3$, as it possesses cubic symmetry over a wide range of temperatures. Its highly symmetric structure simplifies theoretical modeling of transport properties as well as analysis and interpretation of experimental data and it can be viewed as a model system for proton transport in perovskite oxides.

First-principles based density functional theory (DFT) is a powerful tool to extract detailed information about microscopic proton transport mechanisms. Using structure optimization [4–9] and molecular-dynamics approaches [10–13], the stable sites, transition states, and transition pathways of hydrogen in various perovskite oxides have been investigated. It is generally concluded from these simulation studies that the transfer step is slow compared with reorientation, and thereby rate limiting [3,7,11,13]. On the other hand, the strong redshifted OH-stretching mode in experimental infrared spectra is indicative of strong hydrogen-bond interactions, which favor fast proton transfer rather than reorientation, the latter requiring the breaking of such bonds [3]. However, the above simulation studies all treat the nuclei as classical particles. Although attempts have been made to take the quantum nature of the hydrogen motion into account [14–16], a thorough study of the nuclear quantum effects, without resort to quasiclassical approximations, is still lacking. Thus, the nuclei quantum effects, which are likely to be important due to the small hydrogen mass and the high O-H vibrational frequencies, have never been accurately determined.

The path-integral (PI) formulation offers an important way to study the quantum nature of the nuclear degrees of freedom at finite temperature. The combination of path-integral molecular dynamics (PIMD) with electronic structure optimization, the *ab initio* approach, has been used to study various systems [17]; however, few users have considered proton transport in solids and, in particular, proton transport in oxides.

Based on *ab initio* PIMD [18], the present Letter deals with the nuclear quantum effects, such as zero-point motion and tunneling, associated with proton transfer and reorientation in $BaZrO_3$. The *ab initio* PI technique allows the many-body interaction potential to be calculated "on the fly," using contemporary first-principles electronic structure techniques. The thermal and quantal fluctuations are fully accounted for in the interacting many-atom system [19]. This is particularly important for the present system where it is known that the dynamics of the oxygen sublattice is crucial for the proton migration [3] and where quantum effects should be important. Using this method we derive the proton probability distribution over a wide range of temperatures, spanning both the classical and the quantum regimes, and determine the corresponding temperature dependent rates and diffusion coefficient using the path-centroid transition state theory [20]. We find that when the quantum effects are included the reorientation and not the transfer step becomes rate limiting for 600 K and below, in contrast to when the nuclei are treated as classical objects.

The two different elementary steps for proton transport in $BaZrO_3$ are illustrated in Fig. 1. We introduce a reaction coordinate ξ for each process. For proton transfer it is

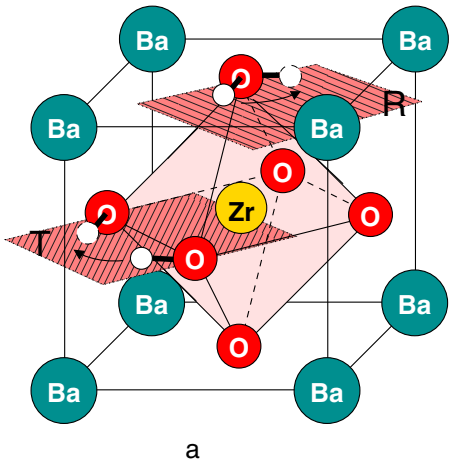

FIG. 1 (color online). Schematic illustration of the proton transfer (T) and reorientation (R) pathways. The small white balls represent the energy minimum position of the proton, and they are equivalent due to the symmetry of the crystal.

chosen as the difference between the two oxygen-hydrogen bond lengths $\Delta R = R_{O_1,H} - R_{O_2,H}$, while for proton reorientation we use the angle Θ between Ba-O-H.

The first-principles calculations were carried out within the framework of DFT employing the generalized gradient approximation (GGA) due to Becke-Lee-Yang-Parr (BLYP) [21]. Using the Car-Parrinello molecular dynamics (CPMD) package [22], with Troullier-Martins norm-conserving pseudopotentials [23], the path-integral (PI) simulations were performed combined with Born-Oppenheimer molecular dynamics. The wave function optimization was performed using a standard iterative subspace method (ODIIS) together with wave function extrapolation for multi k-point calculations. The quantum paths were discretized into $P = 16$ imaginary time slices ($P = 32$ at $T = 100$ K) together with the normal mode transformation with fictitious masses for the noncentroid modes, while Nose-Hoover chain is coupled to each noncentroid nuclear degree of freedom (and one Nose-Hoover chain for the centroid mode) [24]. Most of the computations were performed on a $1 \times 1 \times 1$ supercell containing 1 H and a five-atom $BaZrO_3$ unit. Such a small cell was used as a compromise to reduce the computational cost of the PI simulation. Hydrogen was introduced in the $+1$ charge state and the resulting system was neutralized by the standard means of including a uniform background charge. The setup gave a stable cubic structure with an equilibrium lattice constant $a_0 = 4.13$ Å, which is close to the experimental result $a_0 = 4.19$ Å [25]. Brillouin zone sampling was done using a $3 \times 3 \times 3$ k-point grid and we used the energy cutoff 100 Ry.

To test whether the $1 \times 1 \times 1$ supercell can reproduce the proton properties appropriately, we have computed the classical migration barriers V_m using both the $1 \times 1 \times 1$ supercell and a $2 \times 2 \times 2$ supercell. The barriers were obtained as the differences in total energies with the proton located at the saddle points and at the stable site, respectively. The results are summarized in Table I. We find that the $1 \times 1 \times 1$ cell reproduces the results of the larger supercell quite well. We also find that the present BLYP data agree well with the previous GGA/PW91 results in Refs [8,19].

We first consider the quantum paths. For each quantum path the value of the reaction coordinate $\xi(\tau)$ can be evaluated as function of imaginary time τ. In the MD sampling procedure the centroid $\xi_c = (\beta\hbar)^{-1} \int_0^{\beta\hbar} d\tau \xi(\tau)$ is kept fixed. For each value of the centroid ξ_c we can then determine the corresponding distribution function $P(\xi)$. In Fig. 2 we show the result for $P(\xi)$ with the centroid fixed at the barrier top, $\xi_c = \xi^{\#}$, for the transfer and reorientation process, respectively. The spatial extension of $P(\xi)$ with $\xi_c = \xi^{\#}$ provides qualitative information on the character of the diffusion process. At high temperatures, the distribution approaches the classical limit, $P(\xi) = \delta(\xi - \xi^{\#})$, with no quantum fluctuations. When the temperature is lowered $P(\xi)$ broadens due to quantum fluctuations to a Gaussian shaped function and the diffusion can be viewed more or less as semiclassical overbarrier motion. As can be seen in Fig. 2, this is the situation at 300 and 600 K for both transfer and reorientation. At low temperatures $P(\xi)$ will delocalize with amplitudes towards the two neighboring stable positions. This corresponds to that tunneling processes become crucial for the diffusive motion. This is clearly seen at 100 K, most pronounced for the transfer process.

We next consider the potential of mean force $W(\xi)$, or free energy, for the reaction coordinate ξ. This is evaluated using the constrained molecular-dynamics scheme [26,27] in the blue moon ensemble [26]. The sampling time for the various production runs is 1.5 -4 ps and the length of an equilibration run is of the same order as the corresponding production run. The constrained force evaluation is performed at 7 nonequivalent positions along the reaction coordinate and the force is then integrated to obtain the potential of mean force. This is done both in the classical and quantum cases and in the latter the reaction coordinate ξ is equal to centroid coordinate ξ_c of the corresponding quantum path. Our results are shown in Fig. 3. The classi-

TABLE I. Proton transfer and reorientation barriers calculated with the host lattice atoms fixed at their original positions (fixed lattice) and with the host lattice atoms relaxed to their equilibrium positions in the presence of the hydrogen atom (relaxed lattice) and using two different supercell sizes corresponding to $1 \times 1 \times 1$ primitive cells ($2 \times 2 \times 2$ primitive cells).

Configuration	V_m(eV)			
	Fixed lattice		Relaxed lattice	
Transfer	1.394	(1.313)	0.182	(0.206)
Reorientation	0.337	(0.318)	0.175	(0.182)

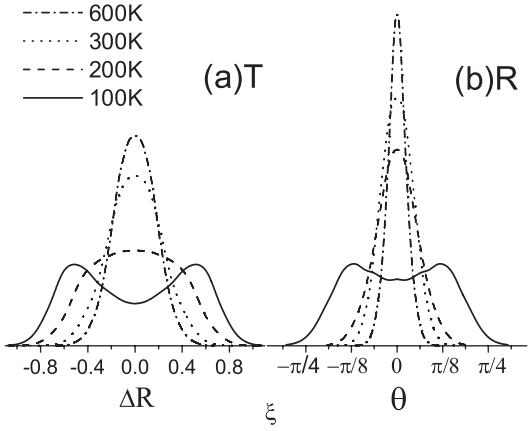

FIG. 2. Temperature dependence of the distribution of the quantum paths $P(\xi)$ with the centroid ξ_c located at the transition state $\xi_c = \xi^{\#}$ for proton transfer (left) and reorientation (right), respectively. The unit of ΔR is Å.

cal free energy barriers are quite similar at the different temperatures (they differ by less than 10 meV) and hence only one of them is presented. The reduction in free energy barrier, as function of temperature, is substantial, in particular, for the transfer process.

Although both transfer and reorientation are elementary migration steps, they are fundamentally different in nature. Proton transfer at the same time involves a process of breaking an O-H bond with one oxygen atom and forming an O-H bond with another. The O-H stretch mode softens significantly during the transfer process and vanishes at the transition state, which reduces the magnitude of the zero-point energy fluctuations and lowers the free energy barrier. However, that is not the case for the reorientation, in which the proton binds tightly to an oxygen during the whole process, and interacts only slightly with the nearest barium atom in the vicinity of the saddle point. Thus the vibrational properties are similar during the entire process and the change of the magnitude of the zero-point energy fluctuations is much less pronounced.

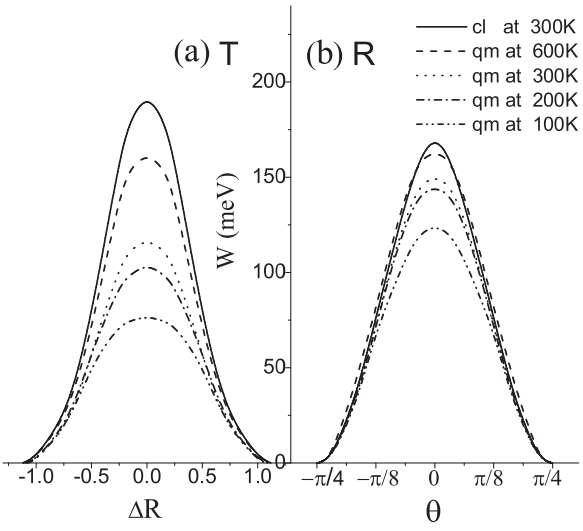

FIG. 3. Temperature dependence of the free energy $W(\xi)$ along the migration path for (a) proton transfer and (b) proton reorientation, both for the classical and quantum cases. The free energy is given as function of (a) the difference of two O-H bonds length $\Delta R = R_{O_1,H} - R_{O_2,H}$ (unit: Å), and (b) the Ba-O-H angle Θ for proton reorientation.

The computed free energies $W(\xi)$ can be used to obtain the corresponding transition rates. In the classical limit we use the classical transition state theory result $k_{cl} = \frac{1}{2} \times \langle | v_\xi | \rangle P_{cl}(\xi^{\#})$, where $\langle | v_\xi | \rangle$ is the average flux of the reaction coordinate at the transition state $\xi = \xi^{\#}$ and $P_{cl}(\xi^{\#}) \propto \exp[-W_{cl}(\xi^{\#})/k_B T]$ is the probability for the system to be located at the transition state, evaluated in the classical limit. In the quantum case we use the path-centroid transition state theory [20] and write the rate as $k_{qm} = \frac{1}{2}\langle | v_\xi | \rangle f_{qm} P_{qm}(\xi_c^{\#})$ where ξ_c denotes the position of the centroid. At high temperatures ($k_B T > \hbar\omega_b/2\pi$) $f_{qm} = 1$ and at low temperatures ($k_B T < \hbar\omega_b/2\pi$) $f_{qm} = 2\pi k_B T/\hbar\omega_b$, where the imaginary barrier frequency ω_b is defined as $\omega_b = \sqrt{\kappa/\mu}$ with $\kappa = -d^2 W(\xi_c)/d^2\xi_c$ and μ equal to the reduced mass for the reaction coordinate ξ_c [26].

The transfer (k_T) and reorientation (k_R) rates are shown in Fig. 4(a). The quantum effects on, in particular, the transfer rate is substantial with an increase of 10^5 at

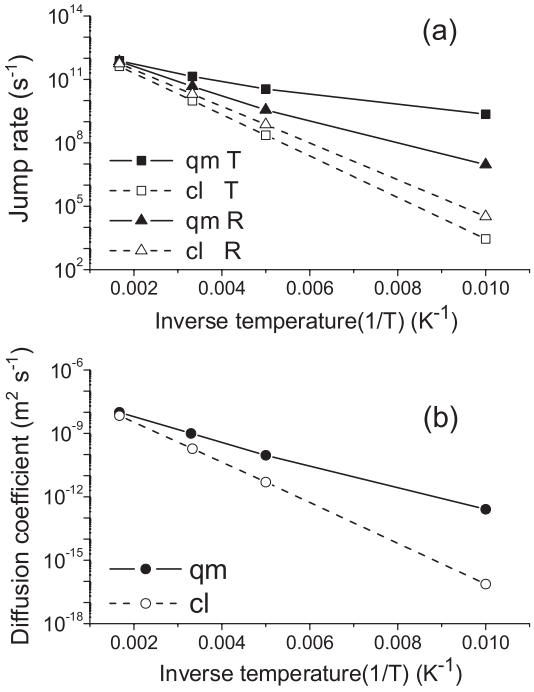

FIG. 4. (a) Proton jump rates for transfer (k_T) and reorientation (k_R) and (b) diffusion coefficient. Solid and dashed lines represent the quantum (qm) and classical (cl) cases, respectively, and T and R denote transfer and reorientation, respectively.

100 K. Both the transfer and reorientation process are necessary for the occurrence of long-range diffusion and the slowest process becomes rate limiting. In the classical case the transfer rate is slower and rate limiting at all temperatures, while in the quantum case the reorientation step becomes rate limiting below 600 K. In Fig. 4(b) we present our results for the diffusion coefficient, which is given by the expression $D = (a^2/6)k_T k_R/(k_T + k_R)$ [28]. In doped $BaZrO_3$ the diffusion rate is reduced by about 2 orders of magnitudes [3], compared with the data in Fig. 4(b), due to the effect of the dopants [9].

In conclusion, the quantum effects on the proton motion in $BaZrO_3$ have been studied using the *ab initio* path-integral molecular-dynamics technique. The full complexity of thermal and quantum fluctuations is thereby included in a natural way for the interacting many-atom system. The migration barriers for the two elementary steps, transfer, and reorientation, have been computed at various temperatures and the corresponding rates and diffusion coefficient are evaluated using the path-centroid transition state theory. In accordance with previous simulations we find that the transfer step is rate limiting when the nuclei are treated as classical point particles. However, when the nuclear quantum effects are included the reorientation step becomes rate limiting below 600 K. Our finding that nuclear quantum fluctuations influence the temperature dependence for hydrogen-bond mediated transfer processes and localized reorientation motion differently will be of importance not only for oxides in general, but also for other systems, e.g., solid acids [29], where the so called Grotthuss mechanism is responsible for the proton transfer process.

This work was supported by the Swedish agencies STINT, NFSM, SNAC, and SSF via the ATOMICS program. Q. F. Z., S. W. G., and E. G. W. were also supported by CAS and NSFC.

*goran.wahnstrom@chalmers.se

[1] H. Iwahara, T. Esaka, H. Uchida, and N. Maeda, Solid State Ionics **3–4**, 359 (1981); H. Iwahara, in *Proton Conductors: Solids, Membranes and Gels—Materials and Devices*, edited by P. Colomban (University Press, Cambridge, 1992), Chap. 8.
[2] K. D. Kreuer, Chem. Mater. **8**, 610 (1996); T. Norby and Y. Larring, Curr. Opin. Solid State Mater. Sci. **2**, 593 (1997).
[3] K. D. Kreuer, Annu. Rev. Mater. Res. **33**, 333 (2003).
[4] F. Shimojo, K. Hoshino, and H. Okazaki, J. Phys. Soc. Jpn. **65**, 1143 (1996).
[5] M. S. Islam, P. R. Slater, J. R. Tolchard, and T. Dinges, Dalton Trans. **19**, 3061 (2004).
[6] C. Shi, M. Yoshino, and M. Morinaga, Solid State Ionics **176**, 1091 (2005).
[7] M. A. Gomez, M. A. Griffin, S. Jindal, K. D. Rule, and V. R. Cooper, J. Chem. Phys. **123**, 094703 (2005).
[8] M. E. Björketun, P. G. Sundell, and G. Wahnström, Faraday Discuss. **134**, 247 (2007).
[9] M. E. Björketun, P. G. Sundell, and G. Wahnström, Phys. Rev. B **76**, 054307 (2007).
[10] F. Shimojo, K. Hoshino, and H. Okazaki, J. Phys. Soc. Jpn. **66**, 8 (1997).
[11] W. Münch, G. Seifert, K. D. Kreuer, and J. Maier, Solid State Ionics **86–88**, 647 (1996).
[12] W. Münch, K. D. Kreuer, G. Seifert, and J. Maier, Solid State Ionics **136–137**, 183 (2000).
[13] M. S. Islam, R. A. Davies, and J. D. Gale, Chem. Mater. **13**, 2049 (2001).
[14] M. Cherry, M. S. Islam, J. D. Gale, and C. R. A. Catlow, Solid State Ionics **77**, 207 (1995).
[15] E. Matsushita, Solid State Ionics **145**, 445 (2001).
[16] P. G. Sundell, M. E. Björketun, and G. Wahnström, Phys. Rev. B **76**, 094301 (2007).
[17] M. E. Tuckerman, D. Marx, M. L. Klein, and M. Parrinello, Science **275**, 817 (1997); R. Rousseau and D. Marx, Phys. Rev. Lett. **80**, 2574 (1998); T. Miyake, T. Ogitsu, and S. Tsuneyuki , Phys. Rev. Lett. **81**, 1873 (1998).M. E. Tuckerman and D. Marx, Phys. Rev. Lett. **86**, 4946 (2001); J. A. Morrone and R. Car, Phys. Rev. Lett. **101**, 017801 (2008).
[18] D. Marx and M. Parrinello, Z. Phys. B **95**, 143 (1994).
[19] D. Marx and M. Parrinello, J. Chem. Phys. **104**, 4077 (1996).
[20] M. Gillan, J. Phys. C **20**, 3621 (1987); G. A. Voth, D. Chandler, and W. H. Miller, J. Chem. Phys. **91**, 7749 (1989).
[21] C. L. Lee, W. Yang, and R. G. Parr, Phys. Rev. B **37**, 785 (1988); A. D. Becke, Phys. Rev. A **38**, 3098 (1988).
[22] CPMD, copyright IBM Corp. (1990–2006), copyright MPI für Festkorperforschung Stuttgart (1997–2001).
[23] N. Troullier and J. L. Martins, Phys. Rev. B **43**, 1993 (1991).
[24] M. E. Tuckerman, D. Marx, M. L. Klein, and M. Parrinello, J. Chem. Phys. **104**, 5579 (1996); G. J. Martyna, M. L. Klein, and M. Tuckerman, J. Chem. Phys. **97**, 2635 (1992).
[25] W. Pies and A. Weiss, in *Landolt-Börnstein: Numerical Data and Functional Relationships in Science and Technology*, edited by K.-H. Hellwege and A. M. Hellwege, New Series, Group III, Vol. 7b1 (Springer-Verlag, Berlin, 1975).
[26] E. A. Carter, G. Ciccotti, J. T. Hynes, and R. Kapral, Chem. Phys. Lett. **156**, 472 (1989).
[27] M. Sprik and G. Ciccotti, J. Chem. Phys. **109**, 7737 (1998).
[28] M. E. Björketun, P. G. Sundell, G. Wahnström, and D. Engberg, Solid State Ionics **176**, 3035 (2005).
[29] S. M. Haile, D. A. Boysen, C. R. I. Chisholm, and R. B. Merle, Nature (London) **410**, 910 (2001).